# PERFORMANCE-SPECTRA BASED METHOD FOR THE SEISMIC DESIGN OF STRUCTURES WITH SUPPLEMENTAL DAMPERS

**J.W.W. Guo & C. Christopoulos**
*University of Toronto, Canada*

**SUMMARY**
A direct design method based on performance-spectra (P-Spectra) for low to medium-rise frame structures with supplemental dampers is presented. P-Spectra are design tools that link multiple damped nonlinear SDOF system responses to the system dynamic and damping properties that structural designers can control. They enable quick comparison of feasible damping solutions without carrying out a detailed trial design. Once a target SDOF solution is chosen, a transformation procedure is used to obtain a MDOF trial damper design that achieves the intended targets with little or no iteration. Numerical verification of the transformation procedure as well as a design example for the seismic upgrade for a 6-storey MRF are presented to illustrate the effectiveness of the proposed method.

*Keywords: performance-based design, supplemental damping, equivalent SDOF*

## 1. INTRODUCTION

The advantages of passive supplemental dampers for performance enhancement of new and existing structures have been demonstrated extensively in past studies. However, current North American guidelines for systems with supplemental dampers (FEMA450) rely on an iterative "analysis method" which focuses on assessing the performance of a trial structure equipped with dampers, but gives limited guidance on comparing different strategies that achieve multiple targeted performance goals. More rational design approaches that target equivalent SDOF response for Lateral Force Resisting System (LFRS) with hysteretic damping (Fu and Cherry 2000, Kasai and Ito 2005, Mansour and Christopoulos 2005, Priestley et al. 2007, Vargas and Bruneau 2009, Lago 2011) and viscous-viscoelastic damping (Kasai et al. 2006a, Kasai et al. 2006b, Priestley et al. 2007, Lago 2011) have been proposed. These studies however, have not established a unified approach for yielding LFRS with both hysteretic and viscous damping that simultaneously accounts for the maximum and residual drifts, force and accelerations, which are all important response quantities that allow for practical performance-based design of structures subjected to multiple performance limits and seismic hazards. This paper proposes a design procedure based on a unified design tool called Performance Spectra (P-Spectra), which link the equivalent SDOF drift, force, acceleration and residual drift to controllable damper and structural properties in a compact format. Direct performance-based design can be performed by transforming P-Spectra SDOF solutions through a systematic procedure, leading to a more efficient design process.

## 2. NORMALIZED RESPONSE OF IDEALIZED SDOF WITH SUPPLEMENTAL DAMPERS

Figure 2.1 shows the backbone curve of idealized SDOF systems with supplemental dampers. The LFRS is idealized as an elasto-plastic system with initial stiffness $K_f$, period $T_f$, and normalized strength $V_f$:

$$V_f = V_{bf}/\left(S_a(T_f)m\right) \leq 1.0 \quad (2.1)$$

where $S_a(T_f)$ and $m$ are the spectral acceleration at $T_f$ and mass of the SDOF system. When $V_f = 1$, the LRFS, herein referred to as the base frame, remains linear elastic.

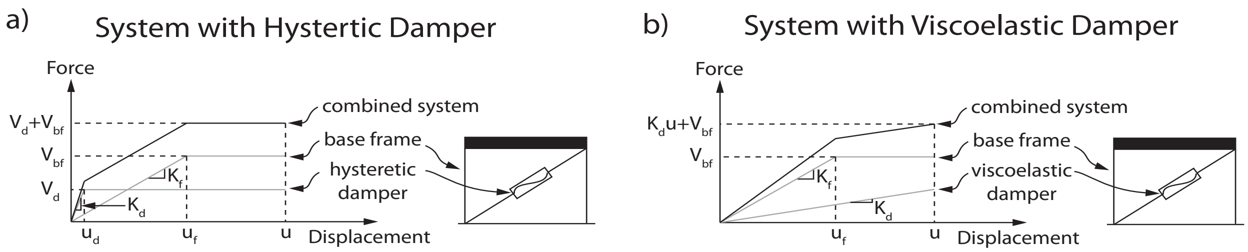


**Figure 2.1**. Idealized backbone curves of systems with a) hysteretic dampers and b) viscous-viscoelastic dampers

Supplemental hysteretic dampers are idealized as elasto-plastic systems having initial stiffness $K_d$ and activation load $V_d$. Supplemental viscous and viscoelastic dampers are idealized as Kelvin solids having stiffness $K_d$ and viscous constant $c$, which can be expressed by the supplemental damping factor:

$$\xi = cT_f/(4\pi m) \quad (2.2)$$

The supplemental stiffness is expressed by the stiffness ratio $\alpha = K_f/(K_f + K_d)$. The ductility $\mu_d$ for the hysteretic damper and $\mu_f$ for the base frame are defined by $u/u_d$ and $u/u_f$, respectively. The ductility $\mu_d$ is set to 1.0 for systems with viscous or viscoelastic dampers. The peak damped displacement and force response normalized to the peak elastic displacement and force of the base frame with natural period $T_f$ are denoted by $R_d$ and $R_a$, respectively. For SDOF systems, the normalized peak force is also equal to the normalized peak acceleration. These quantities are defined as:

$$R_d = D_{damped}/S_d(T_f) \quad (2.3)$$

$$R_a = V_{damped}/\left(S_a(T_f)m\right) = A_{damped}/S_a(T_f) \quad (2.4)$$

where $D_{damped}$, $V_{damped}$ and $A_{damped}$ are the peak displacement, force and acceleration response of the nonlinear SDOF system with dampers. $S_d(T_f)$ is the spectral displacements at $T_f$. Using this response normalization the base frame ductility is given by:

$$\mu_f = R_d/V_f \geq 1.0 \quad (2.5)$$

Finally, for systems with residual displacement $RD_{damped}$, the residual drift ratio $R_s$ is given by:

$$R_s = RD_{damped}/D_{damped} \leq 1.0 \quad (2.6)$$

## 3. PERFORMANCE SPECTRA (P-SPECTRA)

For a given base frame with period $T_f$ and strength $V_f$, the P-Spectra defines the values of $R_a$ and $R_s$ against $R_d$ for systems with hysteretic, viscous and viscoelastic dampers. P-Spectra can be generated using nonlinear time-history analysis (NLA) for an arbitrary ground motion by varying the design parameters $\alpha$, $\mu_d$ and $\xi$. For a suite of ground motions, $S_a(T_f)$ in equation 2.1 is taken as the average spectral acceleration and the normalized responses are averaged over the set of ground motions. Alternatively, P-Spectra can be generated from an equivalent linearization procedure using code-compatible UHS (Guo and Christopoulos 2012). Figure 3.1 shows sample P-Spectra generated using NLA for a system with $T_f = 1$s, $V_f = 40\%$ equipped with hysteretic and viscous-viscoelastic dampers.

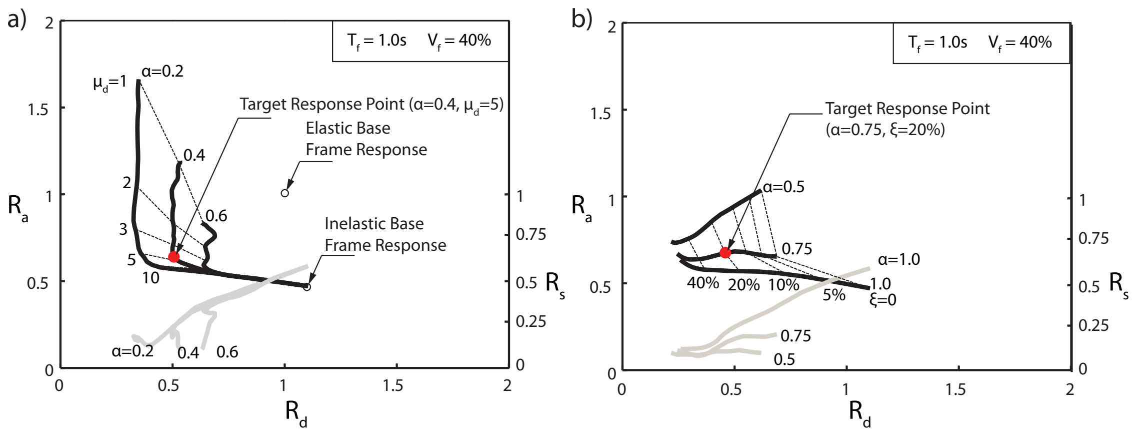


**Figure 3.1**. Nonlinear time-history P-Spectra for a) hysteretic dampers and b) viscous-viscoelastic dampers

In Figure 3.1, the thicker lines in the P-Spectra represent systems with constant $\alpha$ and dotted lines represent systems of constant $\mu_d$ for hysteretic dampers and constant $\xi$ for viscoelastic dampers. The residual ratio $R_s$ is plotted with grey lines and corresponds to the right vertical axis. The elastic base frame response lies at the point defined by $R_a = R_d = 1.0$. The inelastic, undamped base frame response is given by the point at the bottom right of the hysteretic ($\mu_d \to \infty$) and the viscous-viscoelastic ($\alpha = 1, \xi = 0\%$) P-Spectrum. For hysteretic dampers, $R_d$ is mainly controlled by $\alpha$ and $R_a$ is controlled by $\mu_d$. For viscous-viscoelastic dampers, $R_d$ is mainly controlled by $\xi$ and $R_a$ is controlled by $\alpha$. $R_s$ in both cases correlates with the peak displacement $R_d$. Finally, equation 2.6 allow direct considerations of the frame ductility demand in retrofit situations where limits on $\mu_f$ need to be met. Taking advantage of the response trends in different damping systems, the required damper properties can be readily selected from the P-Spectra knowing $T_f$, $V_f$ and the desired values of normalized responses $R_d$, $R_a$ and $R_s$.

Response trends of a given system to different ground motions are immediately obvious on the P-Spectra. Certain ground motions characterized by high energy content at the high frequency range (relative to the natural period of the system) tend to have spectral accelerations that drop off quickly and go into the constant displacement region at relatively low period. In this region, hysteretic damping which modifies stiffness and period is expected to have less effect on the displacement. Figure 3.2 shows the P-Spectra at $V_f$ of 30% and $T_f$ of 1 and 2 seconds for eastern Canadian records (Charette 2009) known for high frequency content and exhibit a transition between constant velocity to constant displacement at lower periods. In such cases, the hysteretic P-Spectrum at 2 seconds shows minor displacement reduction with large increase in shear force compared to the P-Spectrum at 1 second, as expected for this type of dampers. In such cases, viscous and viscoelastic dampers may be preferred because displacement can be controlled by increasing $\xi$. However, as shown by the viscous-viscoelastic P-Spectra at 2 seconds, high shear forces can develop for these records due to the high sensitivity of the viscous force to high frequency contents of the ground motion at large $T_f$ as discussed in (Guo and Christopoulos 2012). Using the P-Spectra for different supplemental damping systems, optimal designs can be chosen to meet specific seismic demand characteristics.

By varying $T_f$ and $V_f$ and arranging the P-Spectra in a matrix as shown in Figure 3.3, complementary stiffening and strengthening can be considered alongside with supplemental damping, which is useful at the preliminary design stage.

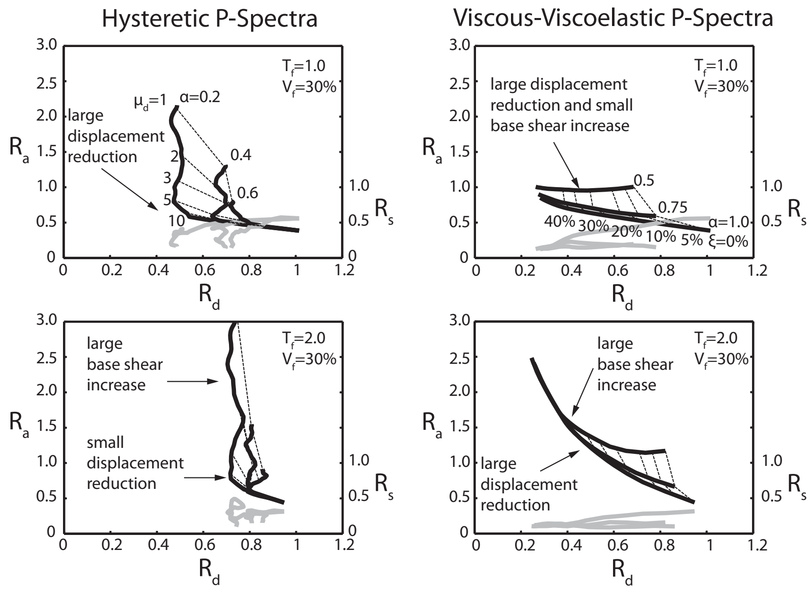


**Figure 3.2**. Hysteretic and viscous-viscoelastic systems under Eastern Canadian records

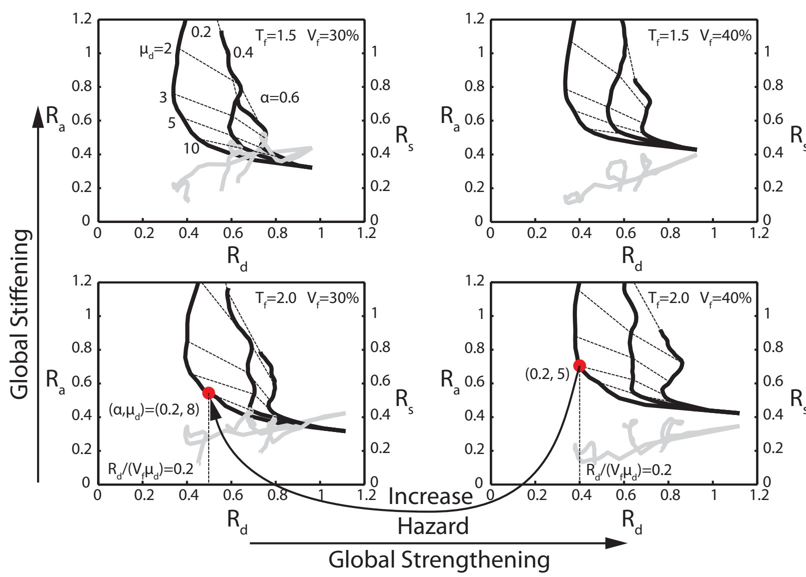


**Figure 3.3**. Hysteretic P-Spectra matrix for stiffening/strengthening and changing seismic hazard

From equation 2.1, scaling the seismic hazard $S_a(T_f)$ up by a given factor scales $V_f$ down by the same factor. Taking advantage of this fact, the response of a particular damping solution can be evaluated at multiple hazards by examining the point on the P-Spectra corresponding to the new $V_f$ having the same hazard-invariants, which are damper properties that are constant with respect to the hazard level. For systems with hysteretic dampers, the hazard-invariants are $\alpha$ and the ratio $R_d/(V_f\mu_d)$, which is proportional to the activation displacement. For systems with viscous-viscoelastic dampers, the hazard-invariants are $\alpha$ and $\xi$. For instance, consider initially a hysteretic system with $T_f = 2s$, $V_f = 40\%$, $\alpha = 0.2$ and $\mu_d = 5.0$. Scaling the hazard up by 33% reduces $V_f$ to 30% and the normalized response under this new hazard is found by maintaining the hazard-invariant properties as shown in Figure 3.3.

## 4. SDOF-MDOF TRANSFORMATION AND HIGHER MODE CONSIDERATIONS

The normalized responses for MDOF structures can be related to the SDOF systems on the P-Spectra defined by $T_f$, $V_f$, $\alpha$, $\mu_d$ and $\xi$ through a transformation procedure that incorporates these parameters, but is otherwise similar to procedures based on the equivalent lateral forces (Fu and Cherry 2000, Kasai and Ito 2005) and proportional damping (Christopoulos and Filiatrault 2006) suggested previously. Further, for dampers with non-zero stiffness, a design mode shape $\{d_i^1\}$ can be chosen to modify the elastic first mode of the damped system. While the final displaced shape is in general not equal to $\{d_i^1\}$ due to inelasticity and higher mode effects, it pushes the system to respond more closely to the desired drift profile. Idealizing the base frame as a shear structure, the equivalent lateral stiffness $K_{f,i}$ can be found by:

$$\begin{aligned} K_{f,i} &= \left(\frac{2\pi}{T_f}\right)^2 \frac{\sum_{j=i}^{n} m_j \phi_j^1}{\Delta\phi_i^1} \\ \Delta\phi_i^1 &= \phi_i^1 - \phi_{i-1}^1;\ \Delta\phi_1^1 = \phi_1^1 \end{aligned} \tag{4.1}$$

where $T_f$ and the fundamental mode shape $\{\phi_i^1\}$ can be obtained from an Eigenvalue analysis of the base frame. For a chosen first mode design mode shape $\{d_i^1\}$ and initial period $T_i = T_f\sqrt{\alpha}$, supplemental damper stiffness can be found by:

$$\begin{aligned} K_{d,i} &= \left(\frac{2\pi}{T_i}\right)^2 \frac{\sum_{j=i}^{n} m_j d_j^1}{\Delta d_i^1} - K_{f,i} \geq 0 \\ \Delta d_i^1 &= d_i^1 - d_{i-1}^1;\ \Delta d_1^1 = d_1^1 \end{aligned} \tag{4.2}$$

For hysteretic dampers, the damper ductility at each storey is set equal to $\mu_d$ of the target SDOF. This assumption implies simultaneous activation of all the dampers under the assumed first mode displacements $\Delta_{d,i}$ and leads to an activation load given by the following:

$$\begin{aligned} V_{d,i} &= \Delta_{d,i}\left(\frac{K_{d,i}}{\mu_d}\right) \geq 0;\ \Delta_{d,i} = R_d \Gamma_D S_d(T_f) \Delta d_i^1 \\ \Gamma_D &= \frac{\sum m_i d_i^1}{\sum m_i \left(d_i^1\right)^2} \end{aligned} \tag{4.3}$$

$\Delta_{d,i}$ in equation 4.3 is the first mode design i$^{th}$ storey inter-storey displacement, and $\Gamma_D$ is the first modal participation factor under this assumed first mode displacement. For viscoelastic dampers, equating the first mode viscous damping ratio at the period $T_f$ gives:

$$c_i = \frac{2\xi M_D \left(\frac{2\pi}{T_f}\right) K_{d,i}}{\sum K_{d,i}\left(\Delta d_i^1\right)^2} \tag{4.4}$$

where $M_D$ is the first modal mass computed using $\{d_i^1\}$. For fluid viscous dampers, no stiffness is added so $K_{d,i} = 0$ and $\{d_i^1\} = \{\phi_i^1\}$. The viscous constants can be calculated using equation 4.4 by replacing $K_{d,i}$ with a fictitious stiffness $\widehat{K_{d,i}}$ computed from equation 4.2 using an arbitrary $T_i < T_f$. Note that $\widehat{K_{d,i}}$ values do not represent real stiffness in viscous dampers, but are numerical tools used to get stiffness proportional damping in the system as discussed in Christopoulos and Filiatrault (2006).

To verify the validity of the SDOF to MDOF transformation, the normalized roof displacement $R_d$ and base shear $R_a$ of idealized 2 to 15 storey shear MDOF designed using equations 4.1 to 4.4 are compared to the target P-Spectra SDOF responses. The verification analysis has been carried out using 10 records from ATC-63 (FEMAP695 2009) scaled to the LA spectrum with $T_f$ from 0.5 to 3.5 seconds, $V_f$ from 10% to 40%, $\alpha$ from 0.2 to 0.6 for hysteretic dampers, 0.5 to 1.0 for viscoelastic dampers, $\mu_d$ from 2 to 6 and $\xi$ ranging from 10% to 30%. The shear MDOF's are assigned storey stiffness computed using equation 4.1 with the first mode shape having constant inter-storey drift along the height. The base shear strength of the shear MDOF's are computed using equation 2.1 at the assumed $V_f$'s. The storey shear strengths are assumed to be proportional to the storey stiffness. The application and verification of this design method to vertically irregular structures is discussed in Guo and Christopoulos (2011). Figure 4.1 shows sample comparisons of $R_d$ and $R_a$ for 9 to 15 storey shear structures with (a) hysteretic and (b) viscous-viscoelastic dampers against the P-Spectra targets. Similar responses are obtained for shorter structures.

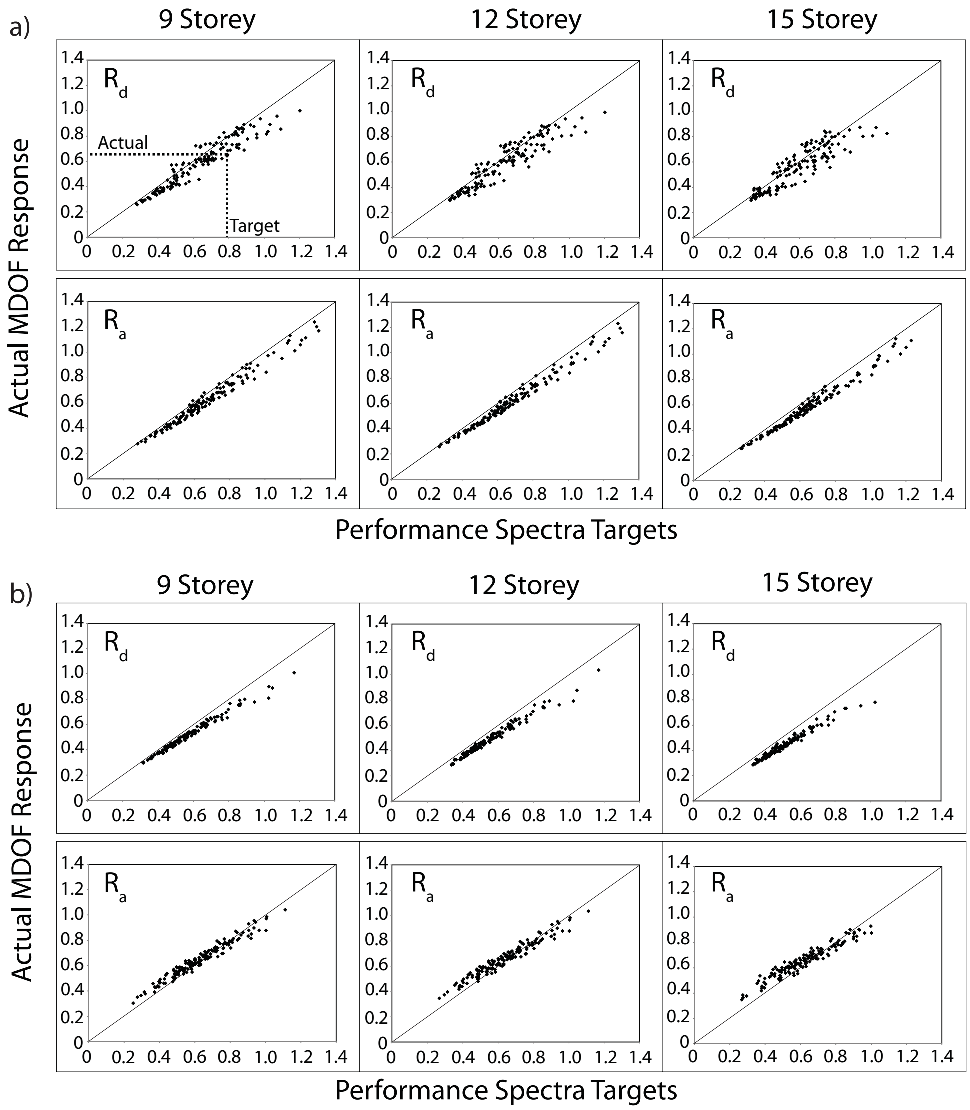


**Figure 4.1**. Actual vs. target response of shear MDOF with a) hysteretic b) viscous-viscoelastic dampers

In general, very good agreement on the global drift and force responses are achieved for all cases. As the number of storeys increases, the accuracy of the P-Spectra predictions decreases due to complex interaction of yielding storeys and higher modes, which can also cause the local storey response to exceed the design targets. A number of methods were proposed to predict the local responses of MDOF's accounting for the inelastic higher modes using modified modal combination techniques (Ramirez et al. 2001, Chopra and Goel 2004, Priestley et al. 2006, Lago 2011, Kreslin and Fajfar 2011). However, these methods involve more elaborate spectral or pushover analysis of the damped MDOF, which is not available in the initial design stage. Hence, similar to Kasai and Ito (2005), the maximum storey response accounting for inelasticity and higher modes is related to the design performance goals by the factor:

$$f_{hx} = \min\left(x_{p,i} / \sqrt{\left(R_x^1 x_i^1\right)^2 + \sum\nolimits_2^{n_m} \left(R_x^m x_i^m\right)^2}\right) \leq 1 \tag{4.5}$$

where $x_{p,i}$ is the performance goal for storey i, $x_i^1$ and $x_i^m$ are the 1st and mth modal response of quantity $x$ found using base frame properties. $R_x^1$ and $R_x^m$ are the 1st and mth modal response modification factors. In equation 4.5, $f_{hx}$ represents the smallest ratio of performance goal to the SSRS response considering the first $n_m$ modes. The modal response $x_i^m$ can be estimated from elastic spectral analysis using properties of the undamped base frame. $R_x^1$ is determined from design performance targets discussed later. $R_x^m$ is set to 1.0 for systems with hysteretic dampers since the effect of hysteretic damping in higher modes is not well defined. For viscous damping, setting $R_x^m$ to 1.0 is very conservative. Assuming the higher modes are linear elastic, the damping in higher modes can be evaluated using:

$$\xi_{eff}^m = \frac{T^m \sum_{i=1}^n \left(c_i \Delta\phi_i^{m\,2}\right)}{4\pi \sum_{i=1}^n m_i \phi_i^{m\,2}} \tag{4.6}$$

where $T^m$ and $\phi_i^m$ are the mth mode period and modal ordinate of the upgraded system. $R_x^m$ may be obtained using P-Spectra at $T^m$, $V_f = 100\%$ and $\xi = \xi_{eff}^m$ or computed using:

$$R_x^m = \exp\left(-1.35 {\xi_{eff}^m}^{0.51}\right) \tag{4.7}$$

Equation 4.7 has been calibrated to extensive time-history analyses of damped SDOF for the purpose of generating P-Spectra using equivalent linearization as discussed in Guo and Christopoulos (2012).

## 5. PROPOSED DESIGN PROCEDURE USING P-SPECTRA

Based on the derivation presented above, a design procedure for buildings with supplemental dampers using P-Spectra is proposed:

1) Set performance targets in terms of drift $\theta_t$, shear force $V_t$, acceleration $A_t$ and residual drift $R\theta_t$.
2) Evaluate the base frame period $T_f$ from Eigenvalue analysis and strength $V_f$ from either plastic analysis or push-over analysis. The influence of $P-\Delta$ should be accounted for.
3) Torsion and vertical irregularity should be checked and accounted for before applying the proposed direct design procedure. Some degree of vertical stiffness/strength irregularity can be tolerated. A more detailed discussion of irregular structures is found in Guo and Christopoulos (2011).
4) Generate P-Spectra using either NLA or a code-compatible equivalent linearization approach described in Guo and Christopoulos (2012). Compute first mode normalized targets:

$$R_d^1 = \theta_t H_{eff} / \left(S_d(T_f)\right) \tag{5.1}$$

$$R_a^1 = \min\left(V_t / \left(M_{eff} S_a(T_f)\right), A_t / \left(\Gamma_f \phi_n^1 S_a(T_f)\right)\right) \tag{5.2}$$

$$R_s = R\theta_t/\theta_t \quad (5.3)$$

where $H_{eff}$ and $M_{eff}$ are the effective height and mass of the base frame. $\Gamma_f$ is the base frame first modal participation factor and $\phi_n^1$ is the base frame roof ordinate of the first mode. Compute $f_{hx}$ using equation 4.5 and multiply $f_{hx}$ by the first mode targets to find the reduced design targets. For systems with viscous damping, $f_{hx}$ can be computed by assuming 15-20% higher mode damping, which should be verified later. Reduced targets are used to select solution(s) on the P-Spectra.

5) Perform SDOF to MDOF transformation using equations 4.1 to 4.4. Design mode shape $\{d_i^1\}$ can be selected for damping systems that add stiffness. A common choice is to use a constant drift profile.
6) Carry out detailed design of dampers and supporting elements. Check capacity for existing frame.
7) Verify trial design using nonlinear time-history analysis (NLA). The responses are expected to be close to the performance targets. Minor refinements are usually required to fine-tune the design.

## 6. EXAMPLE APPLICATION FOR THE UPGRADE OF A 6-STOREY REGULAR MRF

The proposed procedure is illustrated with the preliminary seismic upgrade design for a 6-storey special moment frame designed according to the ASCE-7 (Erochko et al. 2011). Figure 6.1 shows the frame and 10 recorded ground motions (FEMAP695 2009) for LA along with the LA design spectrum. Due to space limitations, this paper only presents the design for the DBE hazard level, which has target drift ($\theta_t$), acceleration ($A_t$) and residual drift ($R\theta_t$) of 1%, 0.5g and 0.5%, respectively. No base shear target was set. The frame period is 1.61s and $V_f$ was found to be 54% using a push-over analysis accounting for $P-\Delta$ effects. The structure has no torsion irregularity and contains very minor vertical irregularity and is hence treated as regular. Using equations 4.5, 5.1 to 5.3, reduced targets are computed and several designs with hysteretic, viscous and viscoelastic dampers that satisfy these reduced targets are examined. Since viscous dampers add damping to higher modes, it was assumed that the 2nd and 3rd mode of the viscous solutions has 15% damping, which is verified later. Two designs, R1 with hysteretic dampers ($\alpha = 0.2, \mu_d = 8, R_d = 0.52, R_a = 0.79, R_s = 0.09,$) and R2 with fluid viscous dampers ($\alpha = 1.0, \xi = 30\%$, $R_d = 0.55, R_a = 0.69, R_s = 0.10$) were chosen since they are the most efficient. For both solutions $\mu_f \approx 1$. R1 is governed by the acceleration limit, which it exceeds by almost 10%. This is accepted at this stage since only an approximate solution is being developed. The required damper properties computed from equations 4.1 to 4.4 are summarized in Table 1. Since hysteretic dampers add stiffness, a design mode shape $d_{Hi}$ with constant storey drift along the height is assumed for R1. For R2, the design mode shape $d_{Vi}$ is taken as the base frame first mode shape because no stiffness is added. Using equation 4.6, the 2nd and 3rd mode of R2 have damping of 73% and 100%, respectively, which greatly exceeds the assumed 15%. For this example, dampers are installed in the middle bay as diagonal braces. It is assumed that the damper can be designed to exactly match the properties given in Table 6.1.

NLA is carried out using OpenSees for the original structure and the upgraded buildings. Figure 6.2 shows the average storey responses along with the performance targets and the amplified design targets for R1 and R2, which are the maximum storey responses amplified using the modified SRSS rule in equation 4.5 with $R_x^1$ taken as $R_d$ and $R_a$ of the selected solutions. Residual drift targets are found by multiplying the storey drift targets by $R_s$. It can be seen that the procedure predict well the maximum storey response based on the P-Spectra normalized responses. Due to slight vertical stiffness irregularity, the drifts are not uniform. Despite this, dampers are distributed as if the system was regular and the SRSS procedure used for $f_{hx}$ still correctly anticipates the maximum inter-storey displacement for design. After the initial design iteration, the drift targets are satisfied except for storey 2 in both R1 and R2, which were slightly exceeded. All acceleration and residual drift targets are satisfied, despite an under-estimation of the peak residual drift for R1 from the modified SRSS combination. Since $R_s$ is only an indicator of the global residual drift, large variations can be expected for storey residuals because they are more prone to higher mode and local inelasticity that are not accounted for in the SDOF analysis. The same is true for the predictions of storey accelerations. On-going investigations are being carried out to address these issues within the context of the proposed method. Finally, the base shears $R_a M_{eff} S_a(T_f)$ are computed for R1 and R2 to be 3660kN and 3320kN, respectively, which are very close to the actual average peak base shears of 3680kN and 3400kN obtained from the NLA.

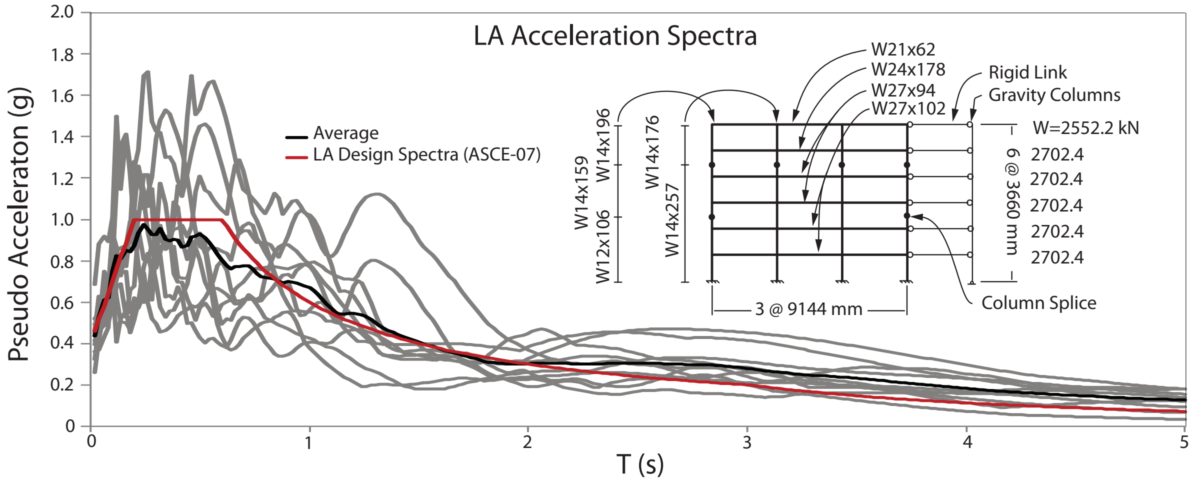


**Figure 6.1**. LA ground motions and description of 6 storey moment frame

**Table 6.1**. Summary of properties of base frame and retrofits R1 and R2

| Storey | Base Frame | | | | | R1 | | R2 |
|---|---|---|---|---|---|---|---|---|
| | $d_{Hi}$ | $\Delta_{Hd,i}(mm)^{(4.3)}$ | $d_{Vi}$ | $\Delta_{Vd,i}(mm)^{(4.3)}$ | $K_f\left(\frac{kN}{mm}\right)^{(4.1)}$ | $K_d\left(\frac{kN}{mm}\right)^{(4.2)}$ | $V_d(kN)^{(4.3)}$ | $c_d\left(\frac{kNs}{mm}\right)^{(4.4)}$ |
| 6 | 1.00 | 28.5 | 1.00 | 19.3 | 33.6 | 85.1 | 303 | 5.2 |
| 5 | 0.83 | 28.5 | 0.88 | 26.0 | 48.2 | 175.1 | 624 | 7.4 |
| 4 | 0.67 | 28.5 | 0.72 | 29.5 | 59.4 | 250.4 | 892 | 9.1 |
| 3 | 0.50 | 28.5 | 0.54 | 33.2 | 63.9 | 306.0 | 1091 | 9.8 |
| 2 | 0.33 | 28.5 | 0.34 | 33.4 | 70.6 | 340.7 | 1215 | 10.9 |
| 1 | 0.17 | 28.5 | 0.14 | 22.3 | 110.1 | 322.2 | 1148 | 16.9 |
| $^{(x)}$ denotes the equation number for which the calculations are based on | | | | | | | | |

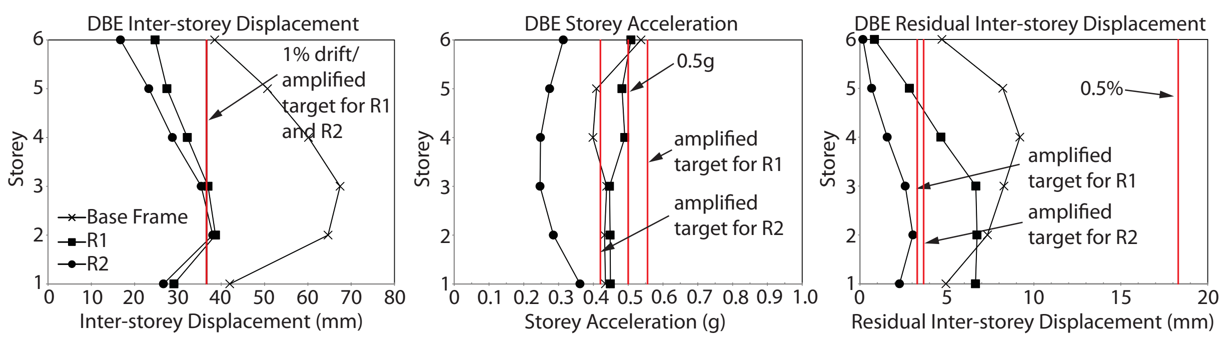


**Figure 6.2**. Average storey drift, acceleration and residual drift responses of R1 and R2 under DBE

## 7. CONCLUSION

A direct performance-based procedure for carrying out the retrofit design of low to medium-rise frame structures using supplemental dampers is outlined. Contrary to the existing "analysis methods", the procedure enables direct assessment of damping solutions that satisfy a given set of performance targets and system constraints in the beginning of the design cycle with minimal computation using graphical tools called P-Spectra. A direct transformation procedure that distributes supplemental dampers to an MDOF from the P-Spectra targets is proposed and verified. The use of the design method is illustrated by upgrading a 6-storey building in LA with supplemental dampers to enhance its seismic performance. Nonlinear time-history results show good agreement of the different response quantities with the performance targets. It was found that the predictions for storey accelerations and residual drifts are generally less accurate than displacements and forces due to influences of higher modes and local inelasticity. Further work is underway to address these issues in the context of the proposed design method.

**REFERENCES**


FEMA450. (2003). NEHRP Recommended Provisions for Seismic Regulations for New buildings and Other Structures. Building Seismic Safety Council National Institute of Building Sciences, Washington D.C, USA.

Fu, Y. and Cherry, S. (2000). Design of friction damped structures using lateral force procedure. *Earthquake Engineering and Structural Dynamics.* **29:7,** 989-1010.

Kasai, K. and Ito, H. (2005). Passive Control Design Method Based on Tuning of Stiffness, Yield Strength, and Ductility of Elasto-Plastic Damper. *Journal of Structural and Construction Engineering.* **595,** 44-55. (in Japanese)

Mansour, N. and Christopoulos, C. (2005). Performance Based Seismic Design of Structures Equipped with Hysteretic Dampers. *Structural Engineering Research Report No. UTCE-05/01*. University of Toronto, Canada.

Priestley, M.J.N., Calvi, G.M. and Kowalsky, M.J. (2007). Displacement-Based Seismic Design of Structures, IUSS Press, Pavia, Italy.

Vargas, B. and Bruneau, M. (2009). Analytical Response and Design of Buildings with Metallic Structural Fuses. I. *Journal of Structural Engineering 2009.* **135:4,** 386-393.

Lago, A. (2011). Seismic Design of Structures with Passive Energy Dissipation Systems. *ROSE School PhD Dissertation.*

Kasai, K., Minato, N. and Kawanabe, Y. (2006). Passive Control Design Method Based on Tuning of Equivalent Stiffness of Visco-elastic Damper. *Journal of Structural and Construction Engineering.* **610,** 75-83. (in Japanese)

Kasai, K., Ogura, T. and Suzuki, A. (2007). Passive Control Design Method Based on Tuning of Equivalent Stiffness of Nonlinear Viscous Damper. *Journal of Structural and Construction Engineering.* **618,** 97-104. (in Japanese)

Guo, J.W.W. and Christopoulos, C. (2012) Performance Spectra-based Design Method for Structures with Supplemental Damping. *Structural Engineering Research Report.* University of Toronto, Canada.

Charette, K.G. (2009). Effets des Mouvement Sismiques sur les Structures en Acier de la Categorie de Constructions Conventionelles. *Dissertation, Ecole Polytechnique de Montreal.* Ecole Polytechnique de Montreal, Canada. (in French)

Christopoulos, C. and Filiatrault, A. (2006). Principles of Passive Supplemental Damping and Seismic Isolation. IUSS Press, Pavia, Italy.

FEMAP695. (2009). Quantification of Building Seismic Performance Factors. ATC-63 Project Report. Applied Technology Council (ATC)

Guo, J.W.W. and Christopoulos, C. (2011). Mitigation of the Seismic Response of Structures with Vertical Stiffness and Strength Irregularity using Supplemental Dampers. *Proc. of the 6th European workshop on the seismic behaviour of irregular and complex structures (CD ROM),* Haifa, Israel.

Ramirez, O.M., Constantinou, M.C., Kircher, C.A., Whittaker, A.S., Johnson, M.W. and Gomez, J.D. (2001). Development and Evaluation of Simplified Procedures for Analysis and Design of Buildings with Passive Energy Dissipation Systems. *Technical Report MCEER-00-0010.* Multidisciplinary Center for Earthquake Engineering Research. University of Buffalo, Buffalo, USA.

Chopra. A. and Goel, R.K. (2004). A modal pushover analysis procedure to estimate seismic demands for unsymmetric-plan buildings. *Earthquake Engineering and Structural Dynamics.* **33,** 903-927.

Kreslin. M. and FajFar, P. (2011). The extended N2 method taking into account higher mode effects in elevation. *Earthquake Engineering and Structural Dynamics.* **40:14,** 1571-1589.

Erochko, J., Christopoulos, C., Tremblay, R. and Choi, H. (2011). Residual Drift Response of SMRFs and BRB Frames in Steel Buildings Designed According to ASCE 7-05. *Journal of Structural Engineering.* **137,** (589).